Canadian Science Publishing | Canadian Journal of Civil Engineering

Using Single and Multiple Unmanned Aerial Vehicles for Microscopic Driver Behaviour Data Collection at Freeway Interchange Ramps

Journal:	*Canadian Journal of Civil Engineering*
Manuscript ID	cjce-2020-0801.R1
Manuscript Type:	Article
Date Submitted by the Author:	11-Mar-2021

Complete List of Authors:	Alamry, Fayez; Carleton University, Department of Civil and Environmental Engineering; Taibah University Yanbu Campus, Department of Civil Engineering Hassan, Yasser; Carleton University, Department of Civil and Environmental Engineering

Keyword:	Traffic Data Collection, Microscopic Driver Behavior Data, Freeway Ramp Terminal, Multiple Unmanned Aerial Vehicles, Traffic Analysis
Is the invited manuscript for consideration in a Special Issue? :	Not applicable (regular submission)

SCHOLARONE™ Manuscripts

Using Single and Multiple Unmanned Aerial Vehicles for Microscopic Driver Behaviour Data Collection at Freeway Interchange Ramps

Fayez Alamry[1, a, *] and Yasser Hassan[2]

[1] **Fayez Alamry**
Lecturer
Department of Civil Engineering
Taibah University
42353, Yanbu, Madinah, Saudi Arabia
email: fmamry@taibahu.edu.sa
[a] Ph.D. Student
Department of Civil and Environmental Engineering
Carleton University
1125 Colonel By Drive
Ottawa, Ontario, Canada, K1S 5B6
Tel: (438) 229-6621
[*] ***Corresponding Author:***
E-mail: fayez.alamry@carleton.ca

[2] **Yasser Hassan**
Professor and Chair
Department of Civil and Environmental Engineering
Carleton University
1125 Colonel By Drive
Ottawa, Ontario, Canada, K1S 5B6
Tel: (613) 520-2600X8625
Fax: (613) 520-3951
E-mail: yasser.hassan@carleton.ca

Word Count: 7979 words + 3 figures + 1 table (each figure and table counted as 250 words) = 8979 words.

Accepted Manuscript Submitted [April 12, 2021]

Abstract

This paper presents a detailed methodological framework for collecting microscopic driver and vehicle behaviour data over a long road segment with an application to the entire stretch of a freeway ramp segment using single and multiple Unmanned Aerial Vehicles (UAVs). The methodology allows users to collect reliable and complete trajectories of traffic movements at areas with challenging physical characteristics (long road segment, horizontal curvature, changing elevation, and presence of shadow), challenging traffic characteristics (high traffic volume, high speeds, and high speed changes), and restrictive regulations (UAVs prohibited from hovering over the freeway or the right-of-way). Different UAV setups were recommended and can be used depending on the site conditions. Specific commercial software and procedures used to complete the data collection are explained. The methodology was applied at two ramps and verified with speed data acquired from differential GPS receivers using three different error metrics. Results showed good performance of the proposed methodology, including when aerial videos must be taken from oblique angles.

Keywords: Traffic Data Collection, Microscopic Driver Behavior Data, Freeway Ramp Terminal, Multiple Unmanned Aerial Vehicles, Traffic Analysis

1. Introduction

Little information is available in the literature about the speeds and behaviour of freeway drivers as they travel along an interchange's ramp and speed change lane (SCL). Most studies (e.g., Ahammed et al. 2008; El-Basha et al. 2007; Yi and Mulinazzi 2007) that examined driver behaviour at freeway ramp terminals observed drivers along the SCL only. Little is also known about the traffic conflicts and interactions that happen between freeway and ramp drivers during the merging and diverging activities. As indicated in the literature (Fitzpatrick and Zimmerman 2007; Torbic et al. 2012), existing knowledge about driver and vehicle merging/diverging behaviour in current North American design guides (AASHTO 2018; TAC 2017) is based on limited studies conducted on passenger cars between the 1930s and 1950s. The design criteria for the freeway SCLs are also based on the laws of kinematics with assumptions related to operating speeds and acceleration/deceleration capabilities of passenger vehicles (Fitzpatrick and Zimmerman 2007; Torbic et al. 2012). Factors such as driver gap acceptance behaviour and the presence of heavy vehicles have not been explicitly considered. Consequently, several researchers have expressed a need to evaluate current SCL design values and called for more research in this area (Fitzpatrick and Zimmerman 2007; Fitzpatrick et al. 2012).

One possible explanation for the lack of driver behaviour data at interchanges is the difficulties in observing vehicles over the entire stretch of a ramp segment in a cost-effective, efficient, and safe manner. Most existing traffic data collection technologies need to be installed on the freeway or within the right-of-way. Typical examples are laser/lidar guns and fixed video cameras; both cannot track all vehicles on all travel lanes at the same time or for a long distance unless multiple units are used. Alternative data collection techniques include using instrumented probe vehicles and driving simulators. However, the accuracy of driving simulators and the sample size required for these studies are two significant concerns. The Naturalistic Driving Study (NDS) conducted through the Strategic Highway Research Program (SHRP 2) can address some of these concerns by collecting the data over a long period of time such that drivers' behaviour will not be altered due to presence of data collection equipment (Dingus et al. 2015). Yet, the equipment cost is another limitation to such studies (Turner et al. 1998).

Unmanned Aerial Vehicles (UAVs), on the other hand, can be a powerful tool for investigating driver behaviour at the microscopic level, specifically in areas where traditional data collection is difficult. Recent research has demonstrated that UAVs can overcome the limitations of traditional data collection methods due to their mobility, flexibility, and ability to cover large areas (Khan et al. 2017a, 2018). Additionally, traffic data captured by UAVs contain more information than those collected by traditional methods (Wang et al. 2016), specifically the non-camera-based methods. Besides traditional data such as speed, density, and flow, UAV videos could provide vehicle-level data, such as lane-change and car-following information (Wang et al. 2016). Combined with image processing tools, the use of UAVs can be a promising technique to provide comprehensive trajectory-based information and driver behaviour at different road segments.

The objectives of this paper are to present a detailed methodology for collecting and extracting accurate vehicle trajectories over a long road segment with challenging physical characteristics using UAVs and video image processing and apply the methodology in a case study to extract trajectories of freeway ramp vehicles and microscopic driver behaviour data over the entire ramp segment. The major tasks covered in this paper include developing a methodology to process UAV videos, collecting aerial video data using single and multiple UAVs, and extracting driver merging and diverging behaviour parameters. The approach adopted for the video analysis consists of three consecutive steps: video stabilization, camera calibration, and vehicle tracking. The methodology was applied at an interchange with two ramps and verified with speed data acquired from differential GPS receivers.

2. UAV Use in Traffic Data Collection

Using UAVs in traffic data collection needs considerable planning and management for efficient use within local laws and regulations (Khan et al. 2017b). For example, Canadian legislations restrict UAV operations for commercial purposes, at nighttime, in adverse weather conditions, and within controlled airspace. Canadian legislations also prohibit UAVs to be hovered over highways or in built-up areas, flown higher than 120 meters above the ground level, or operated within 30 meters of bystanders. These restrictions can prevent recording the videos of traffic movements from optimal top-down camera angles and consequently pose a challenge in employing UAVs in traffic data collection. Another challenge is the UAV's short battery life which makes it difficult to obtain long video footages. Depending on wind conditions and thermal uplift, most of today's commercial UAV batteries, except for much larger and more complicated types, can generally provide 18 to 28 minutes of flight time. A third critical challenge is related to the analysis of UAV videos, which is more complicated than those acquired via stationary camera systems (Khan et al. 2017b). Although most UAVs are equipped with a mechanical stabilizer, UAV footages suffer from camera motions and shakiness, due to wind gusts or vibrations of the UAV's mechanical parts (Khan et al. 2017a). A slight shakiness in the video footage can lead to large errors in vehicles' trajectories, especially when the videos are taken from an oblique angle and long distance (Barmpounakis et al. 2016; Khan et al. 2017a). Moreover, detection of vehicles in aerial videos is still an active research problem in computer vision, mainly due to their small size with regard to the entire frame and potential interference of vehicles close to each other laterally or longitudinally (Maiti et al. 2019).

Yet, considerable research has been recently conducted using a variety of methodological approaches and frameworks for the collection and extraction of vehicle trajectory data from UAV videos. Generally, existing methods to process UAV videos can be classified based on the level of human involvement as manual, semi-automated, and automated image processing techniques. It can be further subcategorized according to the type of vehicle detection algorithm into three types: traditional computer vision, traditional machine learning, and deep learning.

The key advantages of manual and semi-automated video processing techniques, though time-consuming and laborious, are that they are easier to use, can provide highly accurate results, and require less computational power (Khan et al. 2017b). Most related studies in the literature have applied semi-automated computer vision-based techniques to extract kinematic traffic data from UAV video footages (Khan et al. 2017a). For example, Salvo et al. (2014) used UAV video-based data extracted using semi-automated video analysis techniques to investigate driver gap acceptance behaviour at an urban intersection in Italy. The speed data acquired from UAV videos were found to be close to those measured from a differential GPS placed on a probe vehicle. Barmpounakis et al. (2016) conducted a similar UAV-based study to examine vehicles' kinematic characteristics at a low-volume four-leg intersection in Greece. Gu et al. (2019) and Ma et al. (2020) evaluated driver behaviour and safety at an interchange in China based on microscopic traffic data acquired from UAV videos. All previous studies used Tracker, an open-source video processing software developed by Brown and Cox (2009), to extract the positions of individual vehicles from the UAV videos. This software, however, works well only on videos that are taken from a nearly top-down angle or when the direction of vehicle motion is perpendicular to the camera view. These conditions are difficult to satisfy in collecting data over a long segment in most situations due to the regulations concerning UAV operations, as mentioned earlier.

Recently, the advances in computer vision have allowed researchers to consider automatic approaches to process and analyze UAV video data (Apeltauer et al. 2015; Feng et al. 2020; Ke et al. 2020; Khan et al. 2017a; Kim et al. 2019). The main advantage is that automatic video analysis systems can provide quick results with minimum human interactions. However, building a robust and accurate automated video processing system is still a challenging task involving a series of complex algorithms and extensive computational power (Khan et al. 2017b). In addition, traditional computer vision-based systems suffer from limitations such as illumination changes, occlusion, deformation, and background clutter (Shakeel et al. 2019). Khan et al. (2017b) indicated that the accuracy of automatic image processing systems fluctuates with changes in conditions such as light and climate. Moreover, deep learning models, particularly those based on the convolutional neural network (CNN), rely on massive-annotated data and large networks with a large number of parameters (Liu et al. 2020). Annotated image-based datasets are still manually labelled, which is a labour-intensive operation. It was also noted that although deep learning-based detection models offer more accurate and robust results than traditional computer vision-based models, they still have difficulties in detecting vehicles travelling in shaded areas, close to each other, or at far distances from the UAV recording sensor. Most of these issues should be expected on freeway ramps, especially in urban areas where the shadow of nearby trees and fences can deteriorate the reliability of these automated techniques. It is also noted that freeway ramps allow the exchange of traffic movements on grade-separated intersections and are therefore always associated with a change in elevation along each vehicle's path. This adds to the complexity of video processing compared to at-grade intersections, where vehicles are mostly assumed to experience no change in elevation along their paths.

In summary, previous studies using UAVs to collect traffic data have mostly been conducted over small areas such as low-volume intersections using only one UAV in near ideal conditions. Studies that covered longer segments did not include shaded areas or consider geometric characteristics that include horizontal curves or steep grades. Procedures may not be reliably extended to traffic data collection over long and high-speed road segments, especially when the site exhibits challenging characteristics in terms of geometry and shaded areas. Furthermore, legislative restrictions prohibiting UAVs from flying over highways and right-of-way mean that aerial videos can only be taken at oblique angles or at far distances from the area of interest. Therefore, this study covers a gap in UAV data collection research to address these issues and provide a practical and safe methodology to obtain complete and reliable vehicle trajectories over a long segment of high-speed, high-volume road. Applying the methodology to the most challenging area of the freeway, which is the SCL and ramp, would prove the methodology's robustness.

3. Methodology

The methodology adopted in this study is divided into three main phases: data collection, data processing, and trajectory analysis. Figure S1 presents a flowchart of the tasks and tools involved in each phase in addition to data collection using a probe vehicle for comparison with UAV data.

3.1. Phase I: Data Collection

With the aim of developing a methodology that is robust enough to cover long segments of high-speed, high-volume roads with challenging site characteristics, the specific road segment emphasized in this paper is the freeway ramp terminal, including the ramp proper and SCL. As mentioned earlier, this segment has unique features that make UAV videos an ideal tool for traffic data collection but also has features that add to the challenges in UAV video analysis.

In selecting the UAV setup to be used at a specific site, the hovered altitude can first be determined to allow camera coverage of the entire study area, and can be calculated using UAV camera characteristics and the ground dimensions of the study area. However, this altitude must not exceed the maximum allowable altitude according to local regulations or the altitude at which the wind speed does not exceed the maximum UAV's wind speed tolerance, which can be determined by cross-referencing information from weather forecasting services and UAV specifications.

Then, the UAV's hovered location and setup can be determined based on the specific site conditions. As mentioned earlier, an ideal setup is to fly the UAV over the center of the study area and record the videos from a top-down angle. However, because of regulations prohibiting UAVs from flying over highways, Figure 1 illustrates three alternative settings that can be used depending on the site conditions. The figure uses an exit ramp terminal for illustrative purposes, and the same procedures can be used at entrance ramps.

If site conditions permit, Setup 1 (Figure 1a) is the preferred setting using one UAV with the camera positioned such that the paths of SCL vehicles are at an approximately zero horizontal angle from the camera. When a suitable area for UAV takeoff/landing is not available at the same side of the study area, the UAV has to be flown at the opposite side of the study area with the direction of vehicles' paths at an oblique angle to the camera as shown in Setup 2 (Figure 1b). The drawback is that the accuracy of video processing could decrease significantly as the tilt angle and/or the distance between the camera and the vehicles increase. In both setup plans, the camera needs to be positioned such that a portion of the freeway mainline upstream the SCL is covered with the study area to investigate the extent of vehicle deceleration (or acceleration) on the freeway mainline lanes before they diverge off (or after the merge onto) the freeway.

When the study area of interest is relatively large, two UAVs need to be used at the same time, as shown in Setup 3 (Figure 1c). For freeway ramp areas, the first UAV can be set to focus on the freeway mainline and SCL, while the second focuses on the ramp proper. The two UAVs are then set to hover at approximately the same altitude with around 3-5% overlap area while covering the entire study area. One of the main advantages of flying two UAVs simultaneously is that the collected videos would have a high level of details of vehicles and road surface, which would significantly improve the overall accuracy of image processing, especially at low altitudes. An UAV with dual cameras could also be used to cover the study area in Setup 3. However, such an UAV system is currently not available for over-the-shelf use.

Finally, the camera settings and video resolution need to be properly selected based on the expected vehicle speeds (Pueo 2016). Generally, 4k video resolution (3840 × 2160 pixels), 29.97 frames per second (fps) frame rate, and 1/60-second shutter speed would be sufficient for ramp vehicles and virtually all vehicles on a freeway with 100 km/h speed limit. However, a higher shutter speed of 1/120-second is recommended for freeways to capture very aggressively speeding vehicles.

3.2. Phase II: Data Processing

In this phase, the raw UAV videos are processed in three consecutive steps: video stabilization, camera calibration, and vehicle tracking. Each step is a computer vision problem that requires a specific software or algorithm to solve.

3.2.1. Video Stabilization

Video stabilization is the first and most important step in UAV video-based data processing. UAV footages must be properly stabilized before conducting any video analysis as a small shakiness in the UAV footages can dramatically affect the overall accuracy of the extracted traffic information, especially when the footages are taken from a high altitude. Although stabilization features are built in most UAVs, recording videos will still contain some camera shakiness that needs to be removed using digital video stabilization techniques. In this paper, the Mocha Pro software (version 7.50) from BORIS FX and Imagineer Systems Limited was employed to stabilize shaky videos based on a two-dimensional planar motion tracking technique, which is very effective and robust in eliminating camera motions in video sequences. Compared to a point feature matching technique proposed by Khan et al. (2017a), the stabilization process in Mocha Pro is more flexible, quicker, and less sensitive to vehicle movements in the video scene.

The Mocha Pro software requires the user to perform few steps before it can automatically stabilize a shaky UAV video. First, a 2D planar layer must be defined and drawn around objects that remain stationary in all video frames. A mask layer is then added on top of the previous layer to mask out moving objects and ensure that the tracking algorithm only tracks the motions caused by the camera movements. The software then identifies several types of camera motions, including X-Y translation, scale, rotation, and perspective. Once the desired camera motions are chosen by the user, the software tracks each camera motion in every frame and aligns all frames with a reference frame (e.g., the first frame). The software also allows the user to use the tracking data to remove lens distortion and further enhance the video quality.

The level of stabilization can be checked by tracking a stationary point through the video sequences and checking whether its pixel coordinates in the reference frame change between frames. This step can be conducted using an automated point-based tracking algorithm, readily available in Adobe After Effect software or MATLAB computer-vision toolbox. If the output video still contains shaky frames, the stabilization process can be repeated using the output video as the next input video. However, doing so might reduce the quality of the final output video.

3.2.2. Camera Calibration

Camera Calibration is the process of converting image-pixel coordinates into real-world coordinates. Upon reviewing different options for this process, this study used an open-source software called T-Calibration. The software uses the well-known Tasi algorithm (Tsai 1987) to calibrate the camera view (Laureshyn and Nilsson 2018). The software allows users to estimate camera intrinsic and extrinsic parameters, including the camera focal length, principal point, translation, orientation, skew angle, and radial distortion. From these camera parameters, the relationship between the video image coordinates and real-world coordinates can be determined, lens distortions can be corrected, and reliable geometric and dynamic metric information can be derived from the UAV video. The calibration procedure described here can be applied to single or multiple UAVs as each camera is calibrated individually.

The camera calibration using the T-Calibration tool requires two images, which can be two still frames with different camera views or a still frame and a satellite image for the area where the video was recorded. In this study, a still frame from the stabilized video was used along with a satellite image from the open-source satellite imagery platform Google Earth Pro. Figure S2 shows an example of the still frame and satellite image used to calibrate the UAV camera view at one site. It is important that the two images have the same resolution, and the date of the satellite image is close to the date of the video data. To further enhance the calibration process, the satellite image was rectified to the correct map coordinate system using the georeferencing toolbar in ArcMap software (version 10.7) and high-resolution orthoimages normally available through transportation authorities. The orthoimages used in this study were obtained from Carleton University library based on LiDAR data collected by the City of Ottawa between 2015 and 2017. The fundamental vertical accuracy of the used LiDAR data was 8.6 cm, while the ground pixel resolution of orthoimages was 5 cm.

Once the two images are defined in the software, a local X-Y Cartesian coordinate system is placed on the road surface, potentially at the center of the region of interest, and calibrated according to a specific real-world scale. In this study, the origin point (0, 0) of the local Cartesian coordinate system was placed at the start point of the SCL taper for exit terminals or at the painted nose for entrance terminals. The positive X-axis was set in the direction of vehicle motion and the positive Y-axis in the perpendicular direction pointing away from the freeway mainline lanes for exit ramps or towards the freeway mainline lanes for entrance ramps. This setting of the coordinate system ensures that the headings of all exiting or entering vehicles are along the positive X and Y directions.

After defining the coordinate system, the next step is to match and annotate points that are clearly visible in the video frame and satellite image, as demonstrated by the red dots in Figure S2. Common matching points that can be clearly identified in freeway scenes are pavement markings, manholes, and light pole bases. To ensure a high level of accuracy, a sufficient number of matching points need to be annotated and distributed over the entire camera view (Laureshyn and Nilsson 2018). It was noted in this study that using at least 150 matching points for Setup 1 and 2, which were close to each other and distributed over the entire study area, improved the calibration accuracy. In Setup 3 where two UAVs were used and each camera covered a relatively smaller area than the single UAV, 70 matching points for each camera were sufficient to produce a good calibration model.

Traditionally, the true positions of the matching points can be measured directly in the field by a high-accuracy instrument such as Total Station or extracted from high-resolution aerial maps. Because of safety concerns in taking field measurements on freeways, the true positions of the matching points in this study were extracted from the LiDAR and orthoimages. Following Laureshyn and Nilsson (2018) recommendations, the elevations of the measured points were used in the calibration model assuming that vehicles move on a non-flat plane. Once the calibration is completed, the software draws a gird on the camera scene at the center of the Cartesian coordinate system and its projection on the aerial map plane (Figure S2) and displays the average and maximum camera and map errors. Figure S3 shows a heatmap generated by the software for the ranges of the calibration errors in the camera and world planes. Expectedly, the calibration errors increase as the distance from the camera increases.

3.2.3. Vehicle Tracking

The final video processing step is to detect and track individual vehicles in the UAV video sequences. In this study, a semi-automated video analysis software called T-Analyst, which has been used in several traffic-related studies including (Kazemzadeh et al. 2020; Madsen and Lahrmann 2017; van Haperen et al. 2018), was used due to its efficiency, accuracy, and simplicity. The software is also integrated with the calibration software, making video analysis faster and more efficient. Unlike the Tracker software used in other studies, the T-Analyst software allows users to upload and analyze multiple video files even with high-resolution formats, including 4k resolution. Once the stabilized UAV video and calibration model are uploaded into the software, it would allow the user to manually locate the spatial positions of vehicles in the video stream by placing a 3D bounding box around them at regular time intervals, such as every half second (Madsen and Lahrmann 2017). Based on the positions of the 3D bounding box and time interval, the software creates trajectories of each tracked vehicle and determines its speed and acceleration (Madsen and Lahrmann 2017). One of the useful features of this software is that it allows the user to open and work on two video files at the same time, which enhances the process of tracking individual vehicles in Setup 3 as the vehicle moves from one UAV camera view to another. The software also allows the user to estimate vehicles' trajectories along curved segments, which further enhances the accuracy of the extracted data on long segments. Another main advantage of the T-Analyst software is that it allows the user to zoom in to 200% to facilitate the process of tracking vehicles travelling on shaded areas or at far distances from the UAV camera.

In this study, ramp vehicles were tracked every 15 frames (around 0.5 seconds). The smooth function tool within the software was then used to obtain the vehicle trajectory over all frames. This smooth function estimates the X-Y coordinate of the tracked vehicle between the points that were manually tracked every 15 frames using linear interpolation and moving average methods (Monte Malveira 2019). Upon finishing the tracking process, the software allows the user to visualize the accuracy of the tracking process by showing the projection of vehicle trajectories from the video space to the real-world space. The final output of the tracking process is the vehicle's X-Y coordinates, speed, and acceleration in each frame within the tracking area, which can be exported in a tabular format and saved as an Excel file. The same procedure can be followed for extracting trajectories of freeway mainline vehicles.

Two additional steps are needed when using two UAVs (Setup 3). The first step is to match the overlapping trajectories belonging to the same vehicle observed in both camera views. The second step is to connect trajectories from the two UAVs to construct a single complete trajectory of each vehicle across the entire study area. This step requires linking the coordinate systems in the camera views of the two UAVs, which can be achieved by referencing a point of specific physical characteristics such that it is easily identified in both camera views. In this paper, overlapping trajectories of the same ramp vehicle were matched manually. The output data extracted from UAV 1 in the overlapping area can then be evaluated against their corresponding output data from UAV 2 to assess the data accuracy as each camera is calibrated separately. After ensuring that the results in the overlapping area in both cameras are very close, the final values of overlapping points can be taken as the average of the two cameras.

3.3. Phase III: Trajectory Analysis

The final phase in the proposed methodology is the extraction of driver behaviour parameters from the trajectory data acquired from the video processing in the previous phase. As this paper focuses on freeway ramp areas, the driver behaviour parameters of interest include vehicles' speed profiles on freeway mainline lanes and on ramp, acceleration/deceleration on SCLs, merging/diverging speed, merging/diverging location, and accepted merging gaps. All these parameters can be extracted from the vehicle trajectories. For example, by setting the origin point for an exit terminal as the taper starts, as shown in Figure S4a, the diverge point can be identified as the first point in the vehicle trajectory where both the X and Y coordinates are positive. Once the diverge point is found, other parameters can be extracted, such as diverging speed, SCL length utilized, and deceleration rate. The merging point at entrance ramp terminals is determined in a similar way by positioning the origin point at the painted nose.

It should be mentioned that the tracking reference point in the T-Analyst software is the bottom center of the vehicle 3D bounding box that is close to the road surface (Figure S4b). The extracted trajectories can be processed to find the diverging point as the point at which the passenger-side (right) front corner crosses into the deceleration lane or the merging point as the point at which the driver-side (left) front corner crosses into the freeway right lane. Based on this definition, the vehicle's dimensions, which can be extracted from the tracking software, can be used along with the X-Y coordinate of the tracking reference point to determine the X-Y coordinate of the diverge or merge point.

With setting the X-Y coordinate in the way explained earlier as shown in Figure S4 for the case of an exit ramp terminal, the vehicle's heading is always in the first quadrant, i.e., $x_{c2} > x_{c1}$ and $y_{c2} \geq y_{c1}$. The same condition is also satisfied for an entrance terminal with the origin point positioned at the painted nose and the Y-axis pointing towards the freeway mainline lanes. The coordinates of the right front corner (in diverging) or the left front corner (in merging) can then be calculated as:

$$\theta = \tan^{-1}\frac{y_{c2} - y_{c1}}{x_{c2} - x_{c1}} \tag{1}$$

$$x_{f2} = x_{c2} + \frac{L}{2}\cos\theta - \frac{W}{2}\sin\theta \tag{2}$$

$$y_{f2} = y_{c2} + \frac{L}{2}\sin\theta + \frac{W}{2}\cos\theta \tag{3}$$

Where: x_{c1}, y_{c1} = the previous X and Y coordinates of the tracking reference point; x_{c2}, y_{c2} = the current X and Y coordinates of the tracking reference point; x_{f2}, y_{f2} = the current X and Y coordinates of the right front (in diverging) or left front corner (in merging); L = vehicle's length; W = vehicle's width; and θ = vehicle's heading angle.

These equations can be easily applied in Excel or any programing language for the extracted trajectories. The exact frame for the diverge or merge point can then be found when the sign of the Y-coordinate of the relevant vehicle corner changes from negative to positive.

4. Case Study

4.1. Data Collection

The proposed methodology was applied to a case study involving two sites of freeway ramp terminals on Highway 417, Ottawa, Canada, which is a divided multilane freeway with a speed limit of 100 km/h, within the limits of the study area. The two sites were the eastbound (EB) exit and entrance ramps of Parkdale Avenue interchange (Figure S5), which will simply be referred to as the exit and entrance ramps. The annual average daily traffic (AADT) on the freeway's mainline lanes in this area has grown from 163,200 veh/d in 2006 to over 177,000 veh/d in 2016.

The video data were collected in August 2018, during a weekday, in the daytime between 11:00 am to 01:00 pm, and in good weather conditions with the wind speeds at the hovered (recording) altitude not exceeding 7.5 m/s. The UAV videos were captured under these conditions to minimize the effects of shakiness, instability, or shadows in the collected videos, as suggested by Barmpounakis et al. (2016). Moreover, it was important to observe the traffic movements during the off-peak daytime hours to obtain traffic data under free-flow conditions. Such data should reflect drivers' merging/diverging behaviours when not restricted by traffic congestion.

Both selected ramps have a single taper-type SCL. The length of the study area, measured from the traffic signal at the crossroad to the beginning/end of the SCL taper, was 255 and 423 m at the exit and entrance ramps, respectively. The deceleration/acceleration SCL length was measured from the point at which the SCL width is 3.60 m to the ramp controlling feature as defined in AASHTO (2018).

Prior to recording the UAV videos, initial field investigations and reconnaissance were carried out to identify the proper space for the UAV takeoff, landing, and hovering operations. Subsequently, Setup 2 using a single UAV was selected for the exit ramp, while Setup 3 with a pair of UAVs was selected for the entrance ramp. The hovering spot was selected to be as close as possible to the highway and the center of the study area. The UAV takeoff/landing area was selected as close as possible to the hovering spot to minimize the distance and time between the UAV takeoff/landing and hovering and maximize the recording time.

At the exit ramp, the UAV was hovered at 166.73 m altitude, and its spot was 97.13 m away from the takeoff/landing spot, as shown by the yellow line in Figure S5a. The distance between the UAV recording spot and the furthest point in the study area was 363.21 m, as shown by the blue line in Figure S5a. At the entrance ramp (Figure S5b), the recording altitude was 191.60 and 194.45 m, and the hovering spot was 18.02 and 109.45 m away from the takeoff/landing spot, for UAV1 and UAV 2, respectively. The distance between the furthest point of the study area in each camera view and the recording spots of UAV 1 and UAV 2 was approximately 157.70 and 144.63 m, respectively, as shown by the blue lines in Figure S5b.

The flights were carried out by two licensed UAV pilots using two DJI Phantom 3 Professional ready-to-fly quadcopter UAVs. Each UAV was equipped with a 3-axis gimbal stabilization and an advanced camera that can capture a 4k video at 29.97 (fps). Since each UAV had a maximum battery lifetime of around 23 minutes per charge, four additional batteries were used for each UAV to obtain an hour's worth of aerial video. Swapping the UAV batteries was performed nearly after 15 minutes of continuous recordings with a five-minute gap between every two consecutive flights. A total of 126 minutes of aerial video data were collected by the UAVs (65 and 61 minutes at the exit and entrance ramps, respectively). Figure S6 shows sample video footages captured by the UAVs at the exit and entrance ramps.

A probe vehicle was also used to collect GPS-based vehicle trajectories at the exit ramp while the UAV videos were recorded to check the accuracy of the data extracted from UAV videos.

Differential GPS data were collected using two Leica GPS receivers (static and rover receivers). After post-processing, these two GPS receivers provided data at a rate of 10 readings/second and position accuracy in the range of ±1-5 cm for rover operations (Leica 1999). A total of six trips by the probe vehicle were recorded by the GPS and UAV at the exit ramp.

4.2. Results

The collected UAV video data were processed following the data processing phase (Phase II) of the methodology presented earlier on 64-bit Windows 10 platform with an Intel i7-8700K CPU, 64 GB of memory, and Nvidia GeForce GTX 1080 TI. All ramp vehicles were tracked in the UAV footages over the study area using the T-Analyze software. Finally, trajectories of the tracked vehicles were extracted for every frame in the videos and stored in a spreadsheet.

As mentioned earlier, when using two UAVs, the speeds of vehicles in the overlapping area can be used to validate the accuracy of the analysis methodology. Table 1 shows a sample overlapping data for ten randomly selected ramp vehicles observed at the same reference point in both UAV cameras. As shown in the table, the speeds extracted from both UAVs had a maximum difference of 0.8 m/s (3.94%), which indicates that the setup and methodology produced consistent results.

Figure 2 shows sample trajectory data for 10 ramp vehicles at each of the exit and entrance ramps, respectively. Figure 2a and Figure 2c show the space-time diagrams, while Figure 2b and Figure 2d show the speed profiles with the diverge/merge point marked as a circle on each profile. Several driver diverging and merging parameters can be extracted from these figures. For example, the space-time diagram can provide the exact time at which ramp vehicles merged onto the freeway, which can be cross-referenced with the space-time diagram for freeway right lane vehicle to analyze driver’s gap acceptance behaviour. In addition, the speed profiles can be used to analyze the acceleration/deceleration behaviour and diverge/merge speed and location. For instance, Figure 2b shows that drivers at this location tended to diverge off the freeway immediately after the beginning of the SCL taper. The effect of the queue at the traffic light at the crossroad can be observed in the same figure as several diverging vehicles stopped close to the gore nose area. Figure 2d shows that the merging vehicles had significant frequent speed adjustments on the SCL with some vehicles merging at the taper after the end of SCL and that almost all vehicles were still accelerating after they had merged onto the freeway right lane.

4.3. Comparison with GPS Speeds

The performance of the proposed methodology is already evident from comparing the results of the vehicles in the overlap area in Setup 3 that was used for the entrance ramp, as shown earlier in Table 1. The methodology was also evaluated by comparing the UAV-extracted speeds of the probe vehicle at the exit ramp against the GPS speeds, as shown in Figure 3. The UAV measurements (approximately 30 readings per second) were matched with the GPS measurement (10 readings per second) based on the vehicle's geolocation. The average of the 30 readings was then compared with the average of the 10 readings at every one second, as shown in Figure 3. It should be noted that some GPS data were missing in Trips 1, 4, and 5, which is evident in the gaps in the relevant graphs, possibly because of the dense trees and noise barriers near the freeway right lane shoulder, which might obstruct the GPS signals.

In addition to subjective evaluation, three error indicators; Mean Absolute Deviation (MAD), Root Mean Square Error (RMSE), and Mean Absolute Percentage Error (MAPE); were calculated as follows:

(4) $$\text{MAD} = \frac{1}{n}\sum_{i=1}^{n}\left|\text{Probe Vehicle Speed}_{\text{GPS}} - \text{Probe Vehicle Speed}_{\text{UAV}}\right|$$

(5) $$\text{RMSE} = \sqrt{\frac{1}{n}\sum_{i=1}^{n}\left(\text{Probe Vehicle Speed}_{\text{GPS}} - \text{Probe Vehicle Speed}_{\text{UAV}}\right)^2}$$

(6) $$\text{MAPE} = \frac{1}{n}\sum_{i=1}^{n}\left|\frac{\text{Probe Vehicle Speed}_{\text{GPS}} - \text{Probe Vehicle Speed}_{\text{UAV}}}{\text{Probe Vehicle Speed}_{\text{GPS}}}\right| * 100$$

As shown in Table S1, all estimated values of MAD and RMSE were lower than 5 km/h, and all estimated values of MAPE were less than 5%, except for Trip 01. These results confirm that the probe vehicle's speeds obtained from the UAV videos were very close to those measured by the differential GPS method. Generally, RMSE within 5 km/h and MAPE within 5% are considered good results, especially for videos recorded at an oblique angle (Khan et al. 2018).

5. Discussion and Conclusions

This paper proposed a detailed step-by-step UAV-based traffic data collection and extraction methodology. The methodology, which consists of only three steps, can be followed by users who are not versed in UAV operation to collect reliable microscopic traffic data over a long segment of a high-speed, high-volume road, especially when the site has challenging conditions in terms of road geometry (curvature and elevation differences) as well as having significant parts of the segment covered by shadow due to presence of trees and fences. Such difficulties have limited many researchers (e.g., Xu et al. 2020) to only manual video image processing techniques. This paper, therefore, differs from previous UAV-based traffic-related studies in several aspects. First, to allow covering a relatively long segment, the proposed methodology allows for employing single and multiple UAVs to simultaneously videotape traffic over the entire study area. Because of restrictions on UAV operations, aerial videos are captured from camera angles different from optimum UAV camera configuration. Finally, the methodology utilizes manual tracking to allow reliable and accurate extraction of vehicle trajectories in shaded areas or at far distances from the UAV recording sensor. However, a limitation of this study is that the UAV-based video data were collected in the daytime and good weather conditions (no precipitation or strong wind). In addition, the semi-automated approach can be time consuming if the study area has extremely high traffic volumes, which might make the tracking process a difficult task for some users.

A case study was presented where the methodology involving the use of a single and two UAVs was applied to two ramps: entrance and exit. Given that the UAVs used simultaneously on a specific site are calibrated separately, the collected data from both UAVs are independent. Therefore, the extracted speed data at the site covered by two UAVs were compared for vehicles in the overlap area. On the other hand, a probe vehicle was used at the site covered by a single UAV to compare the extracted speed data to GPS-based speeds. The findings revealed the good performance of the proposed methodology, including when aerial videos must be taken from oblique angles. The extracted trajectories for ramp vehicles were shown to be easily manipulated to extract information such as speed profiles, space-time diagrams, and location of diverge/merge point.

Future research will focus on applying the proposed methodology for extracting a sufficient sample of driver and vehicle behaviour parameters at freeway ramp terminals to examine performance of acceleration and deceleration SCL lengths. The data can be used to develop statistical models for driver behaviour parameters at ramp terminals that can be used in other research related to the operational and safety performance or design of ramps and SCL. Examples of studies integrating detailed driver behaviour into the application of freeway SCL design include

(Abdelnaby and Hassan 2014; Fatema and Hassan 2013). It is noted that in all these studies, several assumptions had to be made regarding the drivers' behaviour related to merging or diverging because of lack of reliable data or models to quantify this behaviour.

Acknowledgments

The authors wish to acknowledge Taibah University, Saudi Arabia, for financially supporting this research through the Saudi Arabian Cultural Bureau in Canada.

References

AASHTO. 2018. A Policy on Geometric Design of Highways and Streets. American Association of State Highway and Transportation Officials (AASHTO), Washington, D.C.

Abdelnaby, A., and Hassan, Y. 2014. Probabilistic analysis of freeway deceleration speed-change lanes. Transportation Research Record: Journal of the Transportation Research Board, **2404**(1): 27-37. doi:10.3141/2404-04.

Ahammed, M.A., Hassan, Y., and Sayed, T.A. 2008. Modeling driver behavior and safety on freeway merging areas. Journal of Transportation Engineering, **134**(9): 370-377. doi:10.1061/(ASCE)0733-947X(2008)134:9(370).

Apeltauer, J., Babinec, A., Herman, D., and Apeltauer, T. 2015. Automatic vehicle trajectory extraction for traffic analysis from aerial video data. The International Archives of Photogrammetry, Remote Sensing and Spatial Information Sciences, **40**(3): 9. doi:10.5194/isprsarchives-XL-3-W2-9-2015.

Barmpounakis, E.N., Vlahogianni, E.I., and Golias, J.C. 2016. Extracting kinematic characteristics from unmanned aerial vehicles. Proceedings, 95th Annual Meeting of the Transportation Research Board,Washington, D.C.

Brown, D., and Cox, A.J. 2009. Innovative uses of video analysis. The Physics Teacher, **47**(3): 145-150. doi:10.1119/1.3081296.

Dingus, T.A., Hankey, J.M., Antin, J.F., Lee, S.E., Eichelberger, L., Stulce, K.E., McGraw, D., Perez, M., and Stowe, L. 2015. Naturalistic driving study: Technical coordination and quality control. No. SHRP 2 Report S2-S06-RW-1.

El-Basha, R.H.S., Hassan, Y., and Sayed, T.A. 2007. Modeling freeway diverging behavior on deceleration lanes. Transportation research record: Journal of the Transportation, **2012**(1): 30-37. doi:10.3141/2012-04.

Fatema, T., and Hassan, Y. 2013. Probabilistic design of freeway entrance speed-change lanes considering acceleration and gap acceptance behavior. Transportation Research Recordresearch record: Journal of the Transportation Research Board, **2348**(1): 30-37. doi:10.3141/2348-04.

Feng, R., Fan, C., Li, Z., and Chen, X. 2020. Mixed Road User Trajectory Extraction From Moving Aerial Videos Based on Convolution Neural Network Detection. IEEE Access, **8**: 43508-43519. doi:10.1109/ACCESS.2020.2976890.

Fitzpatrick, K., and Zimmerman, K. 2007. Potential updates to 2004 green book's acceleration lengths for entrance terminals. Transportation Research Record: Journal of the Transportation Research Board, **2023**(1): 130-139. doi:10.3141/2023-14.

Fitzpatrick, K., Chrysler, S.T., and Brewer, M. 2012. Deceleration lengths for exit terminals. Journal of Transportation Engineering, **138**(6): 768-775. doi:10.1061/(ASCE)TE.1943-5436.0000380.

Gu, X., Abdel-Aty, M., Xiang, Q., Cai, Q., and Yuan, J. 2019. Utilizing UAV video data for in-depth analysis of drivers' crash risk at interchange merging areas. Accident Analysis & Prevention, **123**: 159-169. doi:10.1016/j.aap.2018.11.010.

Kazemzadeh, K., Laureshyn, A., Ronchi, E., D'Agostino, C., and Hiselius, L.W. 2020. Electric bike navigation behaviour in pedestrian crowds. Travel behaviour and society, **20**: 114-121. doi:10.1016/j.tbs.2020.03.006.

Ke, R., Feng, S., Cui, Z., and Wang, Y. 2020. Advanced framework for microscopic and lane-level macroscopic traffic parameters estimation from UAV video. IET Intelligent Transport Systems. doi:10.1049/iet-its.2019.0463.

Khan, M.A., Ectors, W., Bellemans, T., Janssens, D., and Wets, G. 2017a. Unmanned aerial vehicle–based traffic analysis: Methodological framework for automated multivehicle trajectory extraction. Transportation research record: Journal of the Transportation, **2626**(1): 25-33. doi:10.3141/2626-04.

Khan, M.A., Ectors, W., Bellemans, T., Janssens, D., and Wets, G. 2017b. UAV-based traffic analysis: A universal guiding framework based on literature survey. Transportation research procedia, **22**: 541-550. doi:10.1016/j.trpro.2017.03.043.

Khan, M.A., Ectors, W., Bellemans, T., Janssens, D., and Wets, G. 2018. Unmanned aerial vehicle-based traffic analysis: A case study for shockwave identification and flow parameters estimation at signalized intersections. Remote Sensing, **10**(3): 458-473. doi:10.3390/rs10030458.

Kim, E.-J., Park, H.-C., Ham, S.-W., Kho, S.-Y., and Kim, D.-K. 2019. Extracting vehicle trajectories using unmanned aerial vehicles in congested traffic conditions. Journal of Advanced Transportation, **2019**. doi:10.1155/2019/9060797.

Laureshyn, A., and Nilsson, M. 2018. How accurately can we measure from video? Practical considerations and enhancements of the camera calibration procedure. Transportation Research Record: Journal of the Transportation Research Board, **2672**(43): 24-33. doi:10.1177/0361198118774194.

Leica. 1999. Technical Reference Manual of Leica's GPS System 500 (version 2.0). Leica Geosystems AG, Heerbrugg, Switzerland.

Liu, L., Ouyang, W., Wang, X., Fieguth, P., Chen, J., Liu, X., and Pietikäinen, M. 2020. Deep learning for generic object detection: A survey. International journal of computer vision, **128**(2): 261-318. doi:10.1007/s11263-019-01247-4.

Ma, Y., Meng, H., Chen, S., Zhao, J., Li, S., and Xiang, Q. 2020. Predicting Traffic Conflicts for Expressway Diverging Areas Using Vehicle Trajectory Data. Journal of Transportation Engineering, Part A: Systems, **146**(3): 04020003. doi:10.1061/JTEPBS.0000320.

Madsen, T.K.O., and Lahrmann, H. 2017. Comparison of five bicycle facility designs in signalized intersections using traffic conflict studies. Transportation research part F: traffic psychology and behaviour, **46**: 438-450. doi:10.1016/j.trf.2016.05.008.

Maiti, S., Gidde, P., Saurav, S., Singh, S., and Chaudhury, S. 2019. Real-time vehicle detection in aerial images using skip-connected convolution network with region proposal networks. International Conference on Pattern Recognition and Machine Intelligence, Springer, Cham.: 200-208. doi:10.1007/978-3-030-34869-4_22.

Mocha-Pro. Software for Motion Tracking and Video Stabilization. Retrieved from: https://borisfx.com/products/mocha-pro. Accessed July 01, 2020.

Monte Malveira, D. 2019. Analysis of Walking and Route-Choice Behavior of Pedestrians inside Public Transfer Stations: A Study on How Pedestrians Behave in the Approaching Vicinity of Level-change Facilities, and How it Affects Their Walking and Route-choice Behavior. (Master' Thesis). School of Architecture and the Built Environment, Civil and Architectural Engineering, Transport planning, KTH Royal Institute of Technology, Stockholm, Sweden. Retrieved from http://urn.kb.se/resolve?urn=urn:nbn:se:kth:diva-264755. Accessed May 01, 2020.

Pueo, B. 2016. High speed cameras for motion analysis in sports science. Journal of Human Sport and Exercise, **11**(1): 53-73.

Salvo, G., Caruso, L., and Scordo, A. 2014. Gap acceptance analysis in an urban intersection through a video acquired by an UAV. Recent Advances in Civil Engineering and Mechanics: 199-205.

Shakeel, M.F., Bajwa, N.A., Anwaar, A.M., Sohail, A., and Khan, A. Detecting driver drowsiness in real time through deep learning based object detection. *In* International Work-Conference on Artificial Neural Networks. 2019. Springer. pp. 283-296.

T-Analyst. Software for Semi-Automated Video Processing. Lund University, Lund, Sweden. Retrieved from: http://www.tft.lth.se/english/research/video-analysis/co-operation/software/t-analyst. Accessed April 01, 2020.

T-Calibration. Software for Camera Calibration. Lund University, Lund, Sweden. Retrieved from: https://bitbucket.org/TrafficAndRoads/tanalyst/wiki/Manual. Accessed April 01, 2020.

TAC. 2017. Geometric Design Guide for Canadian Roads. Transportation Association of Canada (TAC), Ottawa, Ontario, Canada.

Torbic, D.J., Hutton, J.M., Bokenkroger, C.D., and Brewer, M.A. 2012. Design Guidance for Freeway Main-Line Ramp Terminals. Transportation research record: Journal of the Transportation, **2309**(1): 48-60. doi:10.3141/2309-06.

Tsai, R. 1987. A versatile camera calibration technique for high-accuracy 3D machine vision metrology using off-the-shelf TV cameras and lenses. IEEE Journal on Robotics and Automation, **3**(4): 323-344. doi:10.1109/JRA.1987.1087109.

Turner, S.M., Eisele, W.L., Benz, R.J., and Holdener, D.J. 1998. Travel time data collection handbook. Federal Highway Administration, Washington, D.C. FHWA-PL-98-035.

van Haperen, W., Daniels, S., De Ceunynck, T., Saunier, N., Brijs, T., and Wets, G. 2018. Yielding behavior and traffic conflicts at cyclist crossing facilities on channelized right-turn lanes. Transportation research part F: traffic psychology and behaviour, **55**: 272-281. doi:10.1016/j.trf.2018.03.012.

Wang, L., Chen, F., and Yin, H. 2016. Detecting and tracking vehicles in traffic by unmanned aerial vehicles. Automation in construction, **72**: 294-308. doi:10.1016/j.autcon.2016.05.008.

Xu, D., Rouphail, N.M., Aghdashi, B., Ahmed, I., and Elefteriadou, L. 2020. Modeling framework for capacity analysis of freeway segments: application to ramp weaves. Transportation Research Record: Journal of the Transportation Research Board, **2674**(1): 148-159. doi:10.1177/0361198119900157.

Yi, H., and Mulinazzi, T.E. 2007. Observed distribution patterns of on-ramp merge lengths on urban freeways. Transportation research record: Journal of the Transportation, **2023**(1): 120-129. doi:10.3141/2023-13.

Table 1. Summary of comparison of a random sample of vehicles in the overlapping area of the two UAVs.

Vehicle	**Vehicle Speed at the Same Reference Point (m/s)**		**Absolute Difference**	
	Using UAV 1	**Using UAV 2**	**(m/s)**	**(%)**
Vehicle 01	19.00	19.40	0.40	2.08%
Vehicle 02	16.70	17.10	0.40	2.37%
Vehicle 03	18.90	19.10	0.20	1.05%
Vehicle 04	18.60	19.10	0.50	2.65%
Vehicle 05	19.30	19.20	0.10	0.52%
Vehicle 06	19.70	20.10	0.40	2.01%
Vehicle 07	22.90	23.30	0.40	1.73%
Vehicle 08	19.90	20.70	0.80	3.94%
Vehicle 09	20.40	20.40	0.00	0.00%
Vehicle 10	20.60	21.20	0.60	2.87%

List of Figures

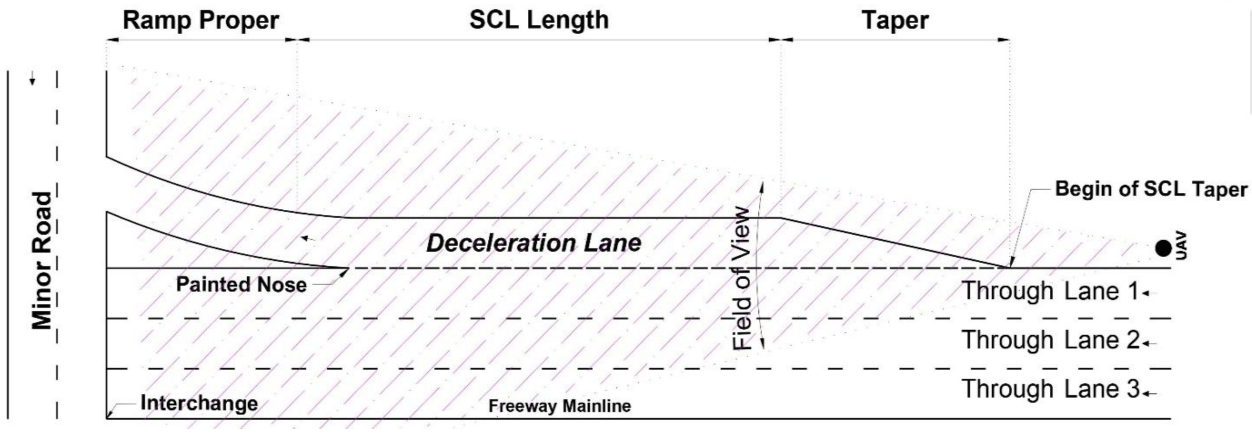

(a) Setup 1

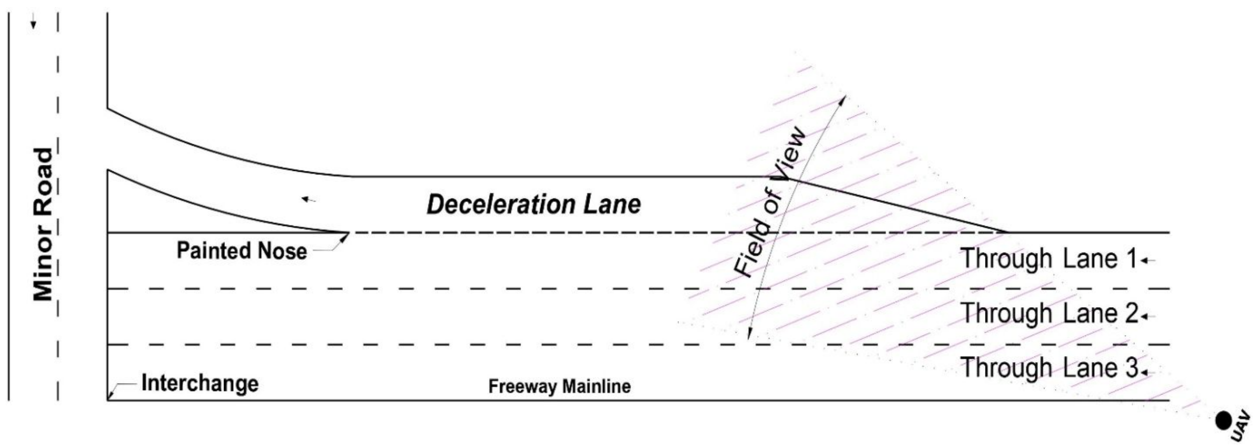

(b) Setup 2

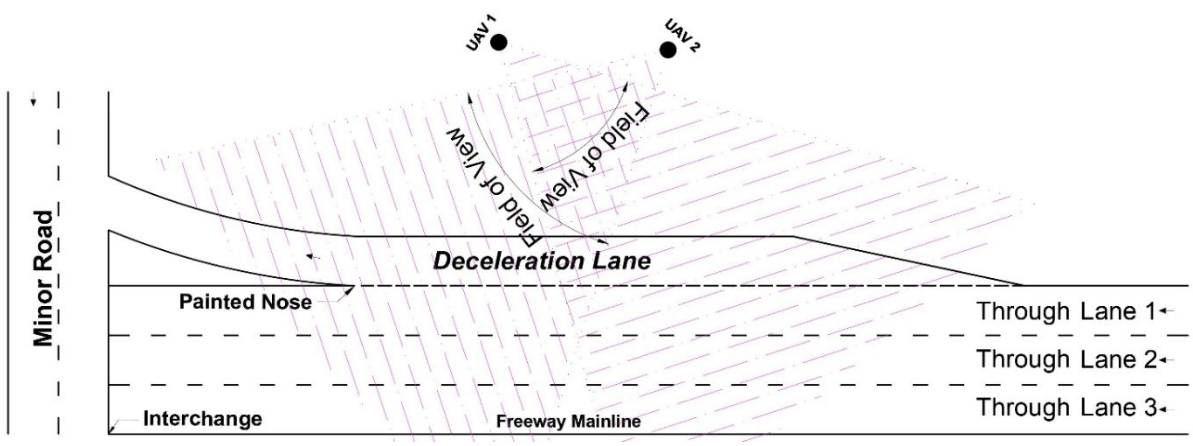

(c) Setup 3

Figure 1. UAV setups and coverage areas.

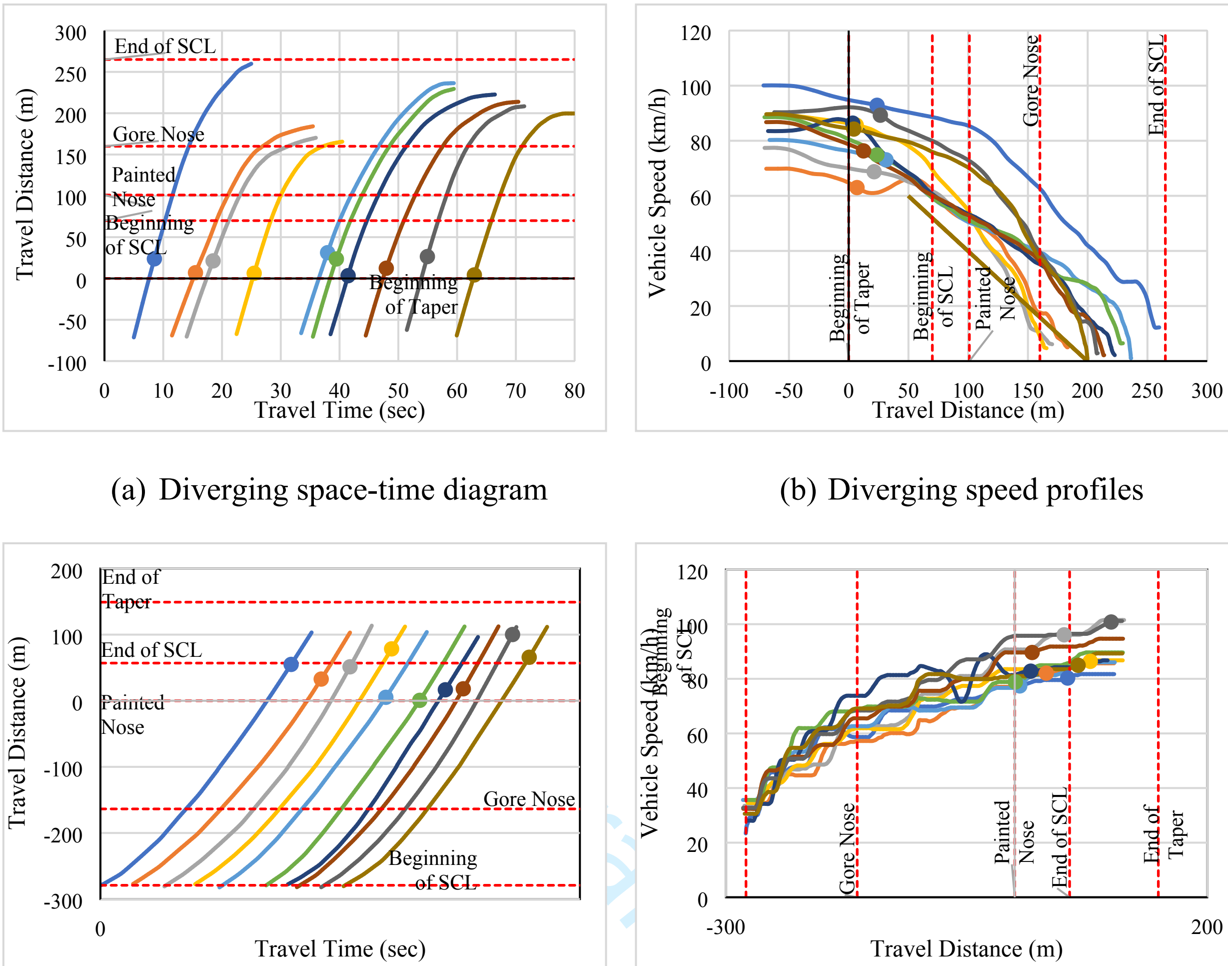

(a) Diverging space-time diagram

(b) Diverging speed profiles

(c) Merging space-time diagram

(d) Merging speed profiles

Figure 2. Driver and vehicle behaviour data.

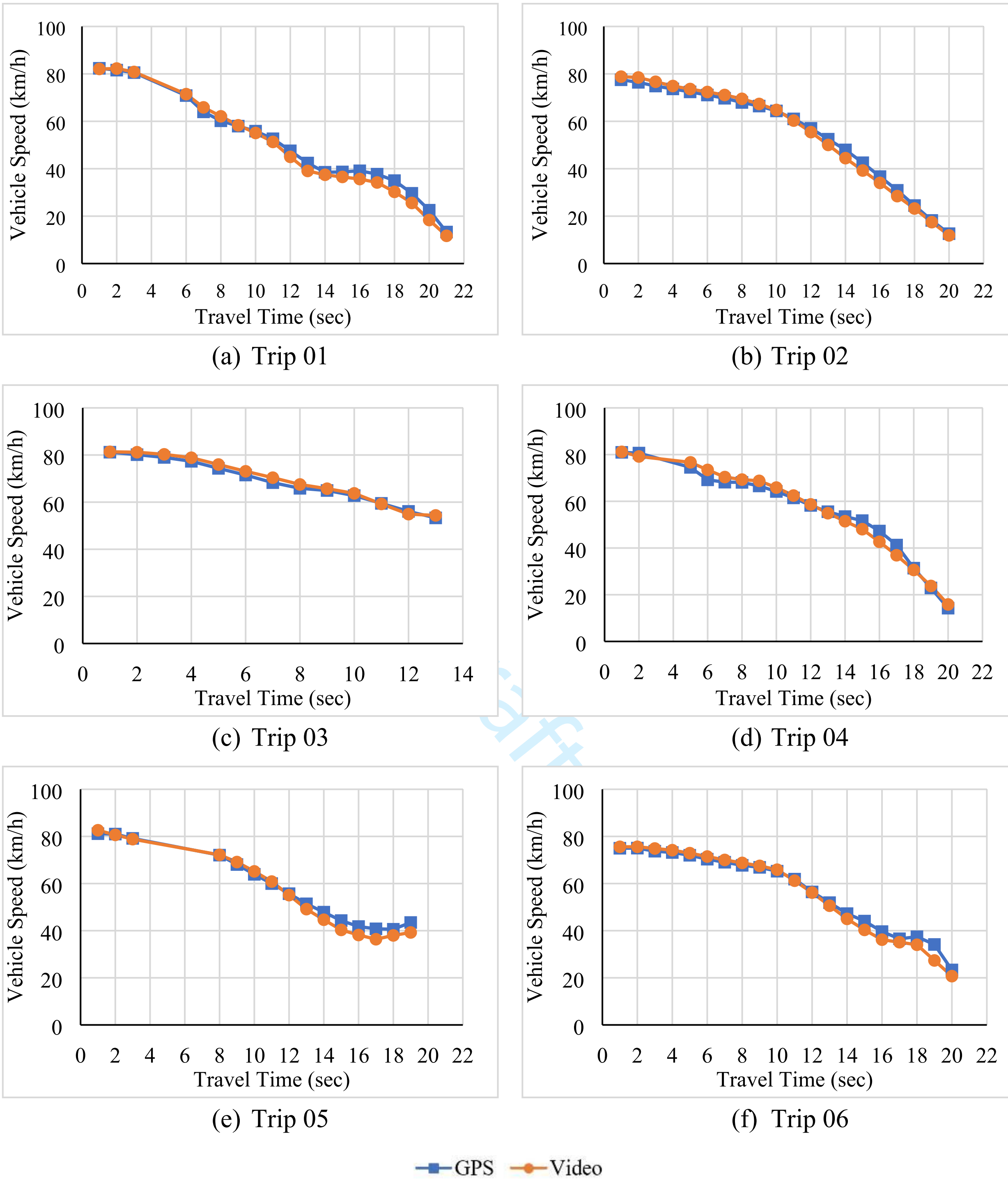

Figure 3. Comparison between probe vehicle's speeds acquired by GPS and UAV.